Rolling contact fatigue

Spalling versus transverse fracture of rails

Steenbergen, Michaël

DOI
10.1016/j.wear.2017.03.003

Publication date
2017

Document Version
Final published version

Published in
Wear

Wear 380-381 (2017) 96–105

Contents lists available at ScienceDirect

Wear

journal homepage: www.elsevier.com/locate/wear

Rolling contact fatigue: Spalling versus transverse fracture of rails

Michaël Steenbergen

Delft University of Technology, Faculty of Civil Engineering and Geosciences, Railway Engineering Group, Stevinweg 1, 2628 CN Delft, The Netherlands

ARTICLE INFO

Article history:
Received 19 July 2016
Received in revised form
17 January 2017
Accepted 9 March 2017
Available online 9 March 2017

Keywords:
Squat
Rail spalling
Stud
White etching layer (WEL)
Rail grinding
Rolling contact fatigue (RCF)

ABSTRACT

Rolling contact fatigue (RCF) defects in the running band of the rail may develop, as a function of born tonnage, either superficially and spall off, or penetrate into the subsurface. In practice, the first type is found to occur notably (but not exclusively) on heat-treated pearlitic rails. Both possibilities involve an essentially different operational risk with respect to transverse rail fracture and require therefore different inspection and maintenance regimes. This study presents a validated hypothesis that explains both similarities and differences of spalling defects and classical squat defects that develop also in depth. It is shown that their microstructural/-mechanical initiation mechanism is different and not necessarily governed by the local tangential stress history in the case of spalling. A model is set up and validated for subsurface crack propagation directivity, distinguishing a spalling and a transverse fracture domain for development of running band defects for both straight track and high and low legs of curves. This model allows for understanding and recognition of the nature of running band defects and for adjustment of control actions.

1. Introduction

Rolling Contact Fatigue (RCF) is a crucial damage mechanism that governs the service life and life cycle costs of the rail in those cases where profile wear is not dominant. RCF can have different forms of appearance, depending on the transverse position at the rail surface and the corresponding local history of the tangential contact stresses exerted by the rolling stock. Notably, head-checks occur on the rail gauge corner and squats in the running band of the rail. Both head-checking defects and leading cracks of squats (see refs. [1,2]) may give rise, in case of uncontrolled growth, to potentially catastrophic rail fracture. Recently however, on the Dutch network an increasing amount of running band defects have been observed that are visually similar to squats, but show a different behaviour: they systematically spall off instead of growing deep into the railhead (Fig. 1). These kind of early defects are found to concentrate on head-hardened rails that have undergone heat treatment during production and perform, during their service life, in the RCF regime. In several cases, an initiation in relation to abusive rail grinding could be established, such as has been discussed in earlier work [4]; however in other cases different factors seemed to govern the initiation process. Similar defects have also been reported in the scientific literature, notably by Grassie and designated by him as 'studs' [5,6]. An example of a longitudinal cross-section through a 'stud' defect with a thermal origination route in the absence of plasticity is shown in Fig. 2.

Although both defects, squats and early spalling defects, are rather similar in appearance and to some extent even in nature – as will be discussed in this paper, both defect types implicate an essentially different operational safety risk. It is therefore of paramount importance to be able to recognise rail defects and the way they develop at an early stage, also in view of adequate maintenance choices, especially as both defect types and differences in their behaviour are known and to some extent also documented in recent literature, but not yet fully understood.

The main contribution of the present work is that it proposes a novel model that explains both differences and similarities in nature between defects that propagate into the subsurface and those that spall off. At the same time the model is capable of predicting the subsurface crack path of surface-breaking RCF cracks in the running band of the rail, distinguishing two spatial propagation domains: a spalling domain and a transverse fracture domain. The proposed model is developed on the basis of earlier work with respect to RCF and squat formation in different track conditions, addressing both microstructural features and three-dimensional crack morphology [7], and on observations on rail defects on the Dutch network.

The structure of this paper is as follows. Section 2 discusses, as a background, properties of spalling defects on the basis of a case study; classical squat defects are not included here as they have been documented in earlier work [1,2,7] and other scientific

E-mail address: M.J.M.M.Steenbergen@tudelft.nl

http://dx.doi.org/10.1016/j.wear.2017.03.003
0043-1648/

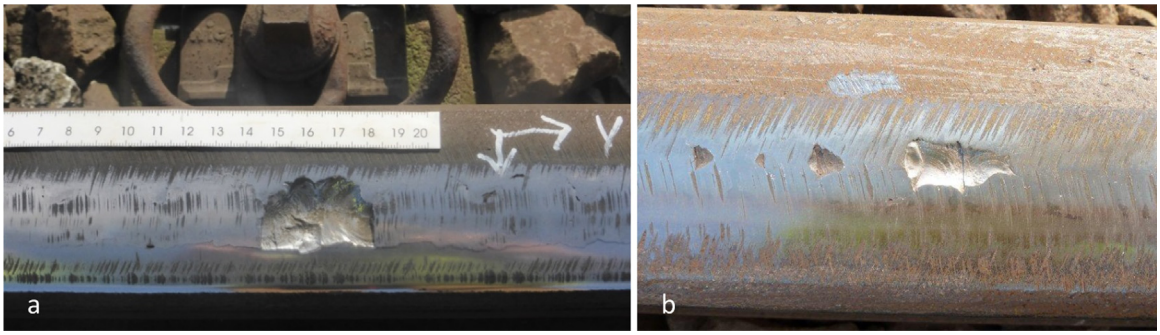

Fig. 1. Spalling defects on grade R370crHT (type MHH) according to classification [3].

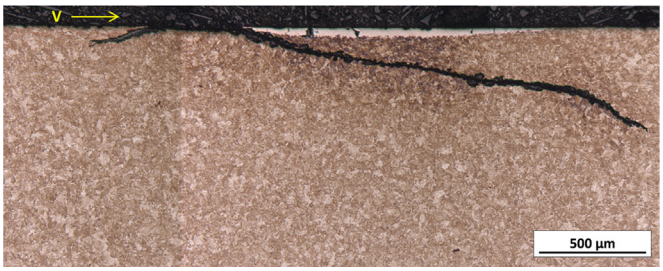

Fig. 2. Longitudinal cross-section over a 'stud' defect on grade R350HT according to classification [3].

literature. Section 3 presents some theory and discussion on surface crack initiation. Section 4 continues with subsurface crack propagation, presenting a model that differentiates between spalling and transverse defect domains. Section 5 discusses, in the framework of model validation, results of microstructural analysis. Section 6 ends with general remarks and conclusions of the work.

2. Case study: spalling defects and their properties in practice

Fig. 3 shows an example of a fully developed individual spalling defect, which, like the defect in Fig. 1a, makes part of a longer, repetitive series of identical defects on heat-treated premium rail in the upper leg of a 2240 m radius curve.

The initiation of such an early defect, in relation to white etching layers along grinding grooves in combination with roughness and harmful residual subsurface stresses induced by a case of abusive maintenance grinding, has been discussed in earlier work [4] and to some extent in the literature on roller bearings [8–10]. Here, the morphology and growth of the defect itself are of interest.

At first view, the geometry of the surface-breaking cracks is striking: the defect shows the 'wedge' shape which is characteristic for squat defects. The crack fronts (Fig. 3a and b) in the subsurface clearly 'expand' from this wedge-shaped surface crack to the other side of the rail. This process would, in the case of squats, give rise to local surface settlement and the development of two 'wings' or 'lobes' in the running band (see for example Fig. 1 in Ref. [7]). However, in this case the wedge opens toward the *field* face of the rail, whereas in the case of squats this opening is systematically toward the *gauge* face [1,7]. Fig. 4 shows another example of a similar spalling defect where this same difference is visible in the crack pattern.

A second observation from Fig. 3 concerns the exact position of the initiation of the defect. Fig. 5 shows in more detail multiple positions of crack initiation: they coincide, both in position and in alignment, with particular grinding grooves. As is particularly clear from Fig. 3c, which shows the surface of the spalled part after polishing with an etching agent (3 percent Nital), after this initiation surface-breaking cracks start to circumscribe the *deepest* area on the rail surface resulting after grinding; a demarcated zone where both individual grinding marks and corrosion are visible due to a lack of contact history under passing wheels. Since this area is the deepest, this means that more material has been removed as compared to the surrounding area, which may suggest the presence of a different (and more harmful) residual stress profile. Fig. 3b shows the internal crack face of the spalled part, where corrosion has started from the position of initiation (the 'oldest' part of the fracture surface), disappearing with increasing distance. A clear distinction is visible between leading and trailing 'wing' of the defect for each individual mechanism, where the term 'mechanism' denotes an individual defect that has fully developed and grown together with its neighbour, forming a defect chain.

It is however interesting to compare the surface-breaking crack path with that which one would expect in the case of regular RCF. Using the model in Ref. [7], one would expect longitudinal shear stresses τ_{zx} opposite to the running direction and transverse shear stresses τ_{zy} toward the gauge face. The leading crack would then initiate perpendicular to the resulting main tensile direction – which is however not the case. This will be discussed (and clarified) further in the following sections. Different causes may, individually or in combination, explain the surface-breaking crack geometry itself, given local initiation at an individual grinding groove:

i. the eventual presence of a differential residual stress profile in the subsurface;
ii. the effect of the geometrical surface irregularity on the response of the material in the top layer of the rail. This comprises a double effect:
   a) inside the moving contact patch, compression occurs in the subsurface, whereas outside this zone tensile stresses occur. The resulting stress alternation at a fixed position yields fatigue, especially if crack initiations are already present.
   b) the occurrence of transient, both normal and tangential contact stress redistribution within the moving contact zone. Such redistribution may lead to cyclic, large tangential stress amplifications along the edges of the deepest surface area with reduced contact stresses, and indeed surface-breaking cracks develop along these edges.

The simulation of effects a) and b) would require extensive and non-conventional modelling work in order to cover both the transient 'interface' effect (distribution of contact stresses, creepage and slip) and its effect on the subsurface stress and strain response. Such modelling work is outside the scope of this study and remains for future work.

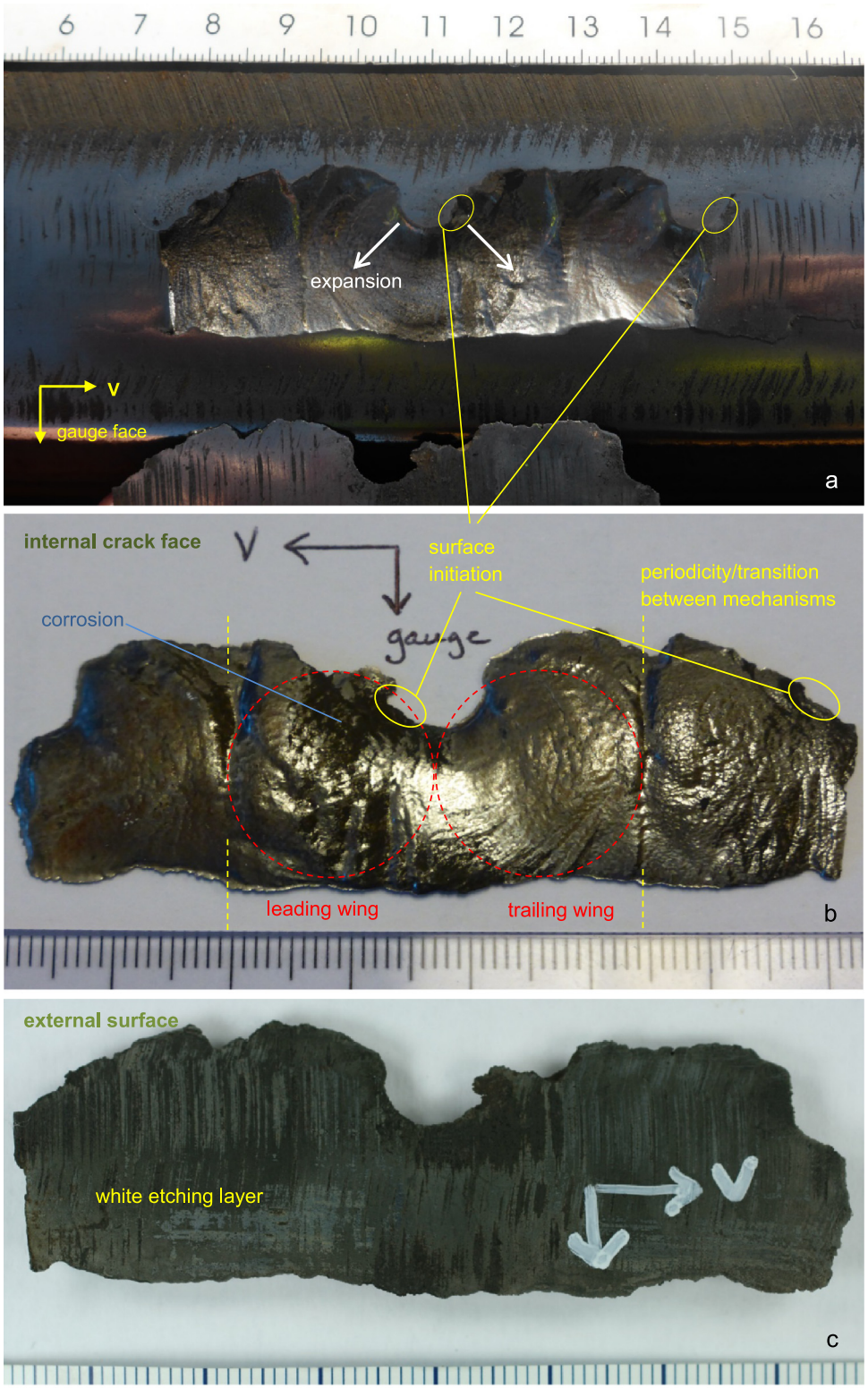

Fig. 3. Spalling defect on grade R370crHT (MHH): top view of the rail with periodic crack pattern; internal crack face and external top view of spalling part (comprising in total 2 'mechanisms').

3. Theory: crack initiation and the surface-breaking crack pattern

In an earlier study into squat initiation [1] (Figs. 13 and 14 in this reference), the growth and orientation of both surface-breaking and subsurface cracks resulting from RCF were addressed. It was established that, for uniform material properties, the orientation of the leading surface-breaking crack with respect to the rail length axis (denoted as the x direction) is determined by the local ratio of the components of the plastic ratcheting tangential stress/strain history, and that crack initiation is most likely to occur at that position at which this local history first reaches a

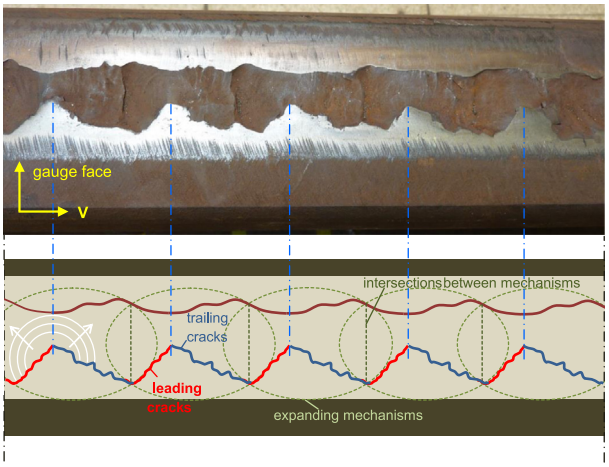

Fig. 4. Fully developed periodic spalling defect (see Ref. [4], Fig. 8b) with serial failure mechanism and schematization.

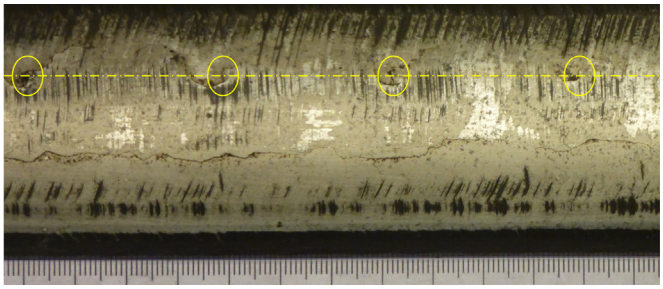

Fig. 5. Surface crack initiation positions of the defects in Figs. 1a and 3.

critical level. This is reached only at the free surface when the friction coefficient over the loading history has been on average larger than approximately 0.3 [11,12]. This knowledge was used as a basis in a further study [7] on squat defects in curves, which proposed for the coordinates of crack initiation $\left(x_i, y_i\right)_{\text{critical}}$ in the running band (where y denotes the transverse direction in the contact plane) an expression for the accumulated composed plastic strain field $R(x, y, t)$. The latter should have a local maximum in the time domain at these coordinates. Local crack initiation may therefore alternatively be described by:

$$\frac{\partial}{\partial t} R\left(x_i^{\text{crit}}, y_i^{\text{crit}}, t\right) = 0;$$
$$R(x, y) = \sqrt{\gamma_{p,zx}^2(x, y) + \gamma_{p,zy}^2(x, y)} \tag{1}$$

Herein, γ_p denotes the plastic shear strain; γ_{zx} the strain component corresponding to the longitudinal tangential stress τ_{zx}, and γ_{zy} the component corresponding to the transverse tangential stress τ_{zy}.

With respect to the subsurface crack propagation of the leading crack of a squat (resulting from RCF and in contrast to the trailing crack), it was established that its growth was determined by the material anisotropy in the top layer of the rail as a result of the accumulated plastic strain field at the moment of crack initiation. In the previous studies [1,2,7] subsurface crack paths were predicted on this basis, with the help of tangential stress expectations for rolling stock, and validated in practice for different track situations.

Eq. (1) presupposes three general conditions with respect to the contact. They concern material aspects, geometry aspects and loading regime aspects. The first condition is homogeneity and three-dimensional isotropy of the material in the top layer of the rail at the onset of the loading process, as well as uniform surface properties (what could also be described as two-dimensional isotropy of an infinitely thin surface layer) throughout the loading process. The second one is 'smooth' contact, i.e., both contacting surfaces do not experience geometrical deviations that affect the global contact stress distribution over the full contact area (which does not include e.g. micro-roughness required for adhesion); one may also say that the nominal and the real contact area coincide. The third condition is stationarity/monotony of the loading regime; i.e., the parameters that govern the individual loading case do not change significantly throughout the loading history. Although in many cases these three conditions are met, or at least met sufficiently so that deviations do not affect the damage behaviour, they are not generally given in wheel-rail contact. Specific examples are:

a) the presence of a top layer on the rail with different chemical and/or constitutive properties as compared to the subsurface material. Typical examples are surface layers with pro-eutectoid (hypoeutectic or free) ferrite (Fig. 6), resulting from decarburisation during the manufacturing or heat treatment process of pearlitic rails, or with hypereutectic grain boundary cementite in the case of higher carbon content. Decarburised layers typically exhibit reduced tensile strength and fatigue resistance and are detrimental to wear and fatigue life (see refs. [13–15]);
b) surface effects of grinding in the form of deposits of hard and brittle friction-induced martensite (FIM), subsurface anisotropy [4,16] and macro-roughness containing wavelengths of the same order of magnitude as the dimensions of the contact patch;

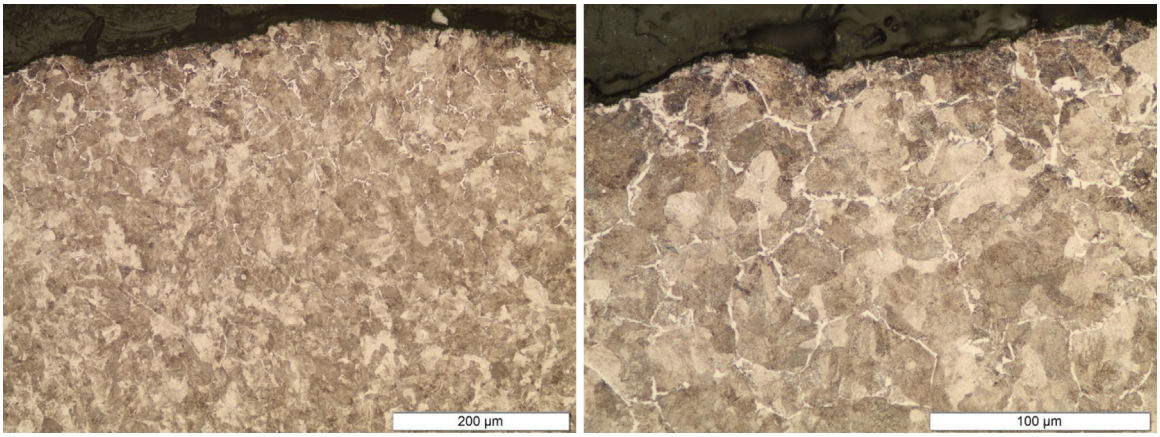

Fig. 6. Example of decarburisation (pro-eutectoid or free ferrite, visible as a white phase along the grain boundaries) in the surface layer of rail grade R350HT.

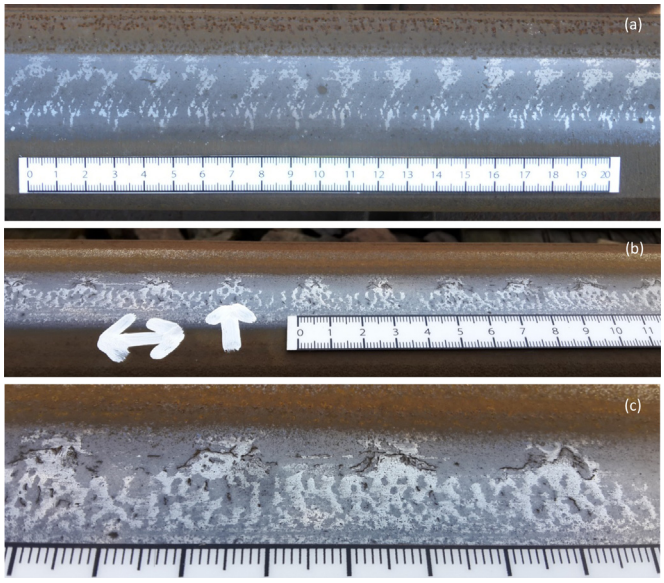

Fig. 7. Non-uniform WEL at the rail surface (R260Mn on straight track) (a,b,c); associated to surface cracking (b,c (close-up)) (*photos b-c: courtesy Gijs Brefeld*).

c) the presence of a WEL on the rail surface and associated residual stresses, due to effects such as increased microslip in a continuous high traction/adhesion operating regime;
d) the presence of cracks and eventually local settlements in the rail surface, which may give rise to stress redistribution within the contact area and a difference between the nominal and the real contact patch. A typical example is the brittle trailing crack of a squat defect, caused by the presence of the leading RCF crack [7,17];
e) variation in operating conditions, such as a varying or even substantially modified friction coefficient and a change in vehicle types and parameters (such as axle load, traffic direction, wheel profile, driven versus non-driven axles).

In all the cases a) though e), the given factors may dominate with respect to 'normal' RCF and govern crack initiation as well as the surface-breaking crack behaviour, which is then no longer in accordance with the model proposed in Ref. [7]. An example for case c) is given in Fig. 7, which shows two cases of clearly observable non-uniform WEL on a rail, one of which is associated to surface cracking. The WEL has formed under a loading history with bi-directional train operation at high traction/adhesion levels with significant microslip/creepage. It is also noted that the mentioned factors that cause a deviation from the general situation may interact. This occurs in the case of generation of a non-uniform WEL as a result of locally increased micro-slip in the presence of significant contact roughness. Such a case is exemplified in Fig. 8.

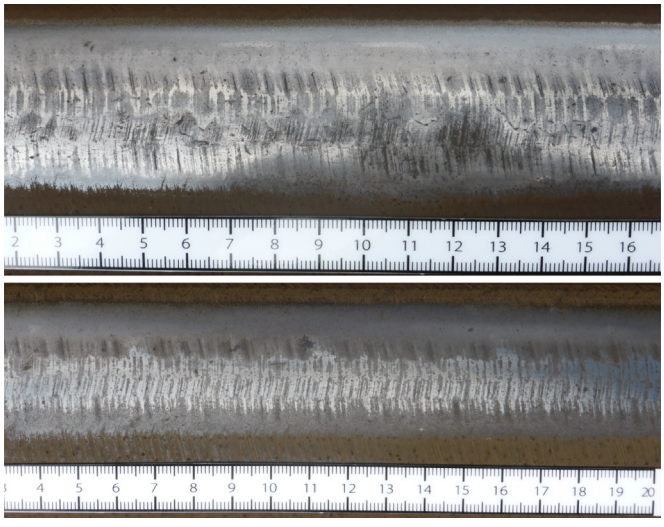

Fig. 8. Non-uniform WEL in the running band of the rail (R260Mn on straight track) associated to macro-roughness of the surface and consecutive train operation.

In the previous, it has been established that there are cases in which the surface-breaking crack geometry is different from the one that could be expected for 'regular' RCF. The question remains what is the effect on the further subsurface crack growth. This is the topic of the next section. In general, it can be said that the present study enlarges the scope of the model in ref. [7] for those situations in which the layout of the surface-breaking crack and the disposition of the subsurface (its 3D texture) by the tangential stress history do not 'match'.

4. Crack propagation model: 'transverse defect' versus 'spalling' domains

On the basis of what has been discussed in the previous section, a model can be made that predicts the nature of a rail defect (spalling or developing into a transverse defect) independent of the specific cause of the surface-breaking crack, given the local tangential loading history (or its prevailing part) and the orientation of the surface-breaking crack. Fig. 9 illustrates the 3D anisotropy of the subsurface that occurs under tangential stresses corresponding to one-directional train operation on a straight track (assuming a friction coefficient larger than 0.3, or first yield at the surface) according to the model in ref. [7] for prediction of squat crack morphology. Fig. 9 shows, distinguishing in a similar manner as in this work straight track and high/low legs of curves, spalling and transverse defect (TD) domains of internal crack propagation. Independent of the track situation there are three quarter-planes (or quarter-spaces) in which subsurface crack propagation leads to a spalling defect and one quarter-plane yielding transverse failure. Application of this scheme to a situation with a given surface-breaking crack geometry then allows to conclude in which domain the defect will develop.

The above can be illustrated for the defect shown in Fig. 3 and discussed in Section 2. The result is depicted in Fig. 11, showing the orientation of a surface-breaking crack under regular RCF for this case, the direction (quarter-space) of subsurface crack propagation

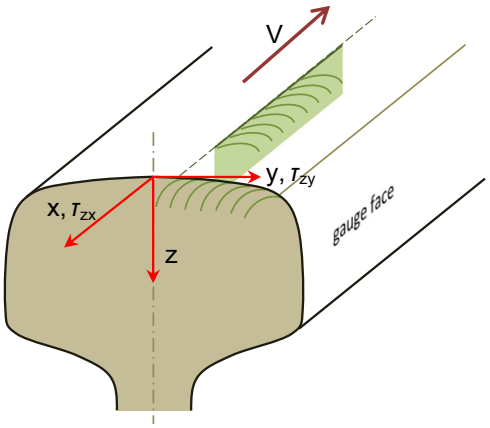

Fig. 9. Coordinate system and subsurface anisotropy due to tangential stress directivity and a plastic ratcheting response (straight track situation, operation in one direction).

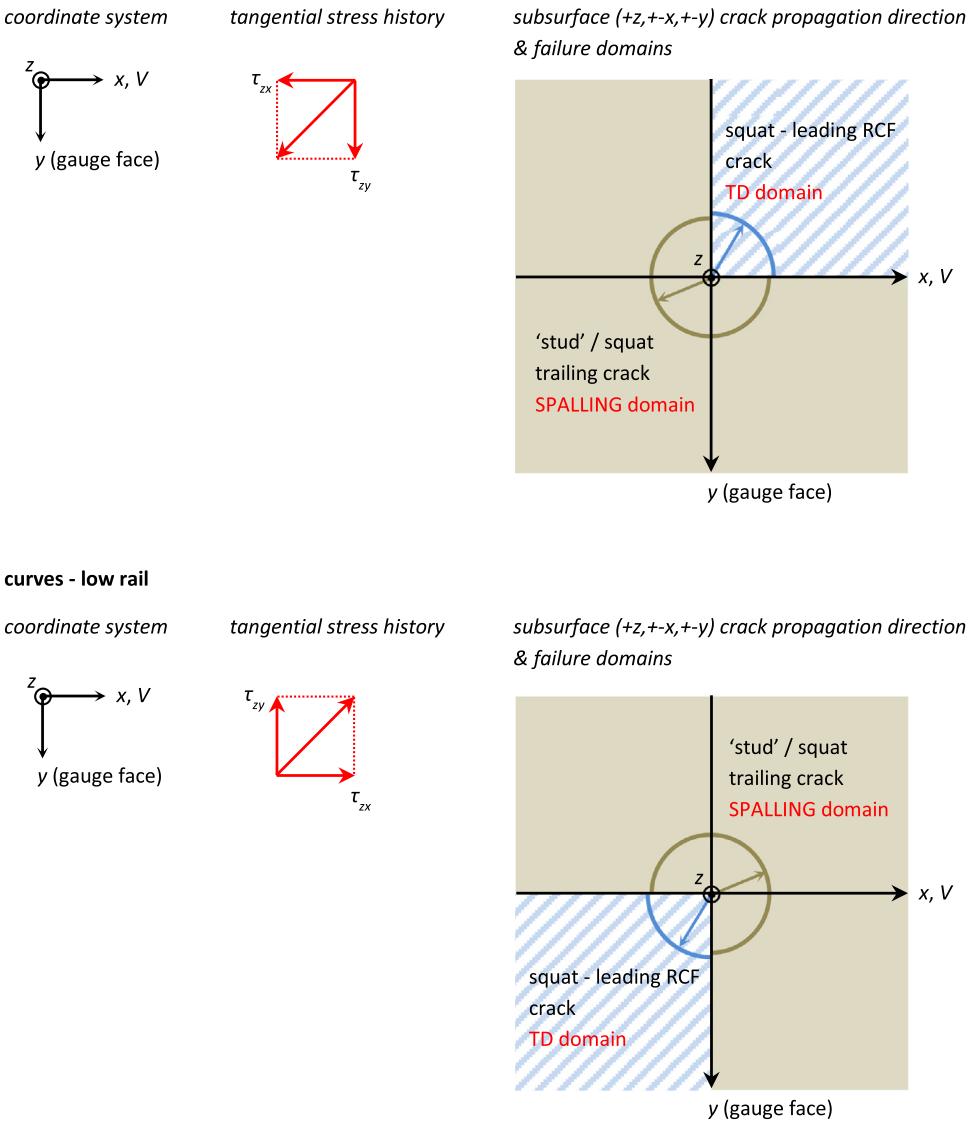

Fig. 10. Transverse defect (TD) versus spalling domains (quarter-spaces) for surface-breaking cracks in the running band of the rail in different track situations, assuming one-directional train operation.

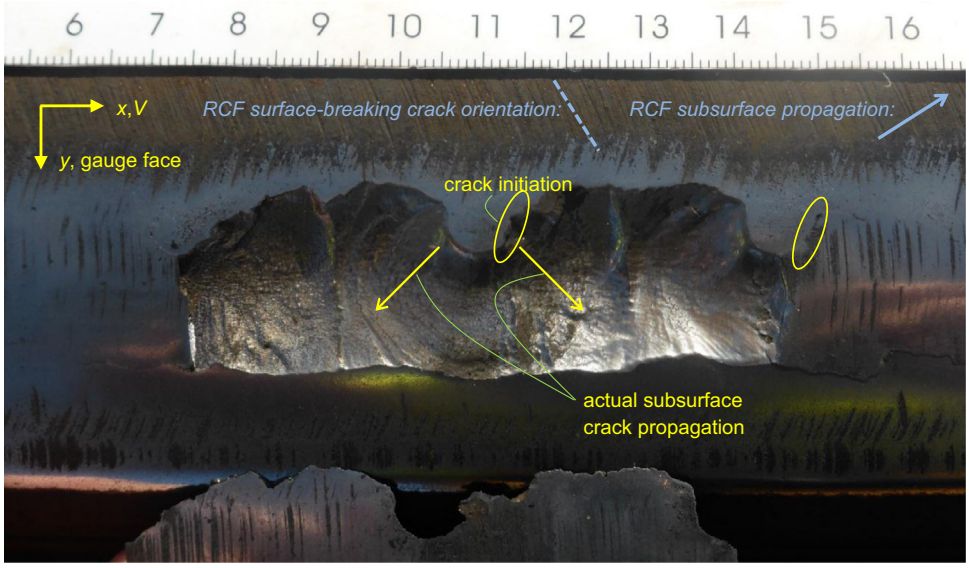

Fig. 11. Spalling defect on R370crHT (MHH) in the upper leg of a 2240 m radius curve (see Fig. 2).

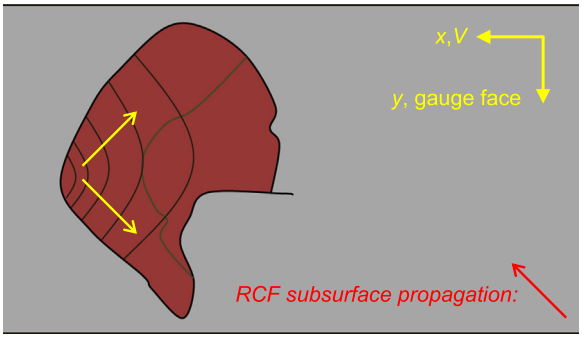

Fig. 12. Spalling defect in Ref. [6] and interpretation according to the model in Fig. 10.

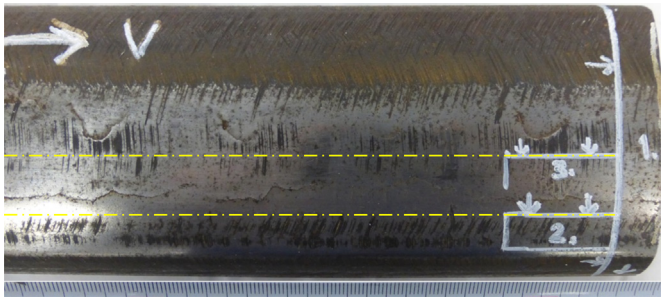

Fig. 13. Examined cross-sections (1–3) along the surface of the defect zone.

leading to a TD defect in accordance with the scheme of Fig. 10, and on the other hand the actual surface-breaking crack initiation line and both internal actual propagation directions. Because the surface-breaking crack orientations do not match, *both* subsurface crack planes are situated in the spalling domain. The defect is therefore not a conventional case of RCF/squat formation and will not (or is not able to) lead to a transverse rail defect. This is, as has been mentioned in the introduction, an important conclusion in view of the essential difference in operational safety risk, and therefore the required monitoring and maintenance actions.

The model can, in the same way, also be applied to results reported in the literature. Fig. 1 in ref. [6] shows a spalling defect ('stud'). From the figure the location of surface-breaking crack initiation remains unclear (though most likely at the left in the centre of the running band) and it is questionable whether it is unique (multiple grinding marks are visible). However, the subsurface propagation directions (quadrants) are very clear from the fatigue marks and reproduced in Fig. 12, which also shows the RCF subsurface propagation quadrant according to the scheme (upper part) in Fig. 10. It is clear that the defect has developed entirely in the spalling domain, is therefore not a classical squat defect and represents a negligible risk with respect to rail fracture.

Both cases that have been discussed show that the scheme in Fig. 10 can be a useful tool not only for analysis and understanding, but also to assess the risk of existing running band defects with respect to rail fracture and therefore safe train operation and the need of maintenance.

In the framework of this study it is interesting to return to the trailing crack of squat defects. It has been addressed both in earlier work [1,2,7] and in the literature (for example ref. [17]), and the question has been posed why the leading crack of a squat is always critical with respect to the – eventual – trailing one. The theory developed in this study provides an explanation: the leading crack develops in the TD domain and the trailing crack in the spalling domain.

5. Microstructural analysis

In order to further clarify the application of the model of Fig. 10 to the spalling defect considered in the case study in Section 2 of this paper, additionally a microstructural analysis has been performed of an individual defect from the series. Fig. 13 shows the concerned part of the defect and the examined cross-sections, comprising a transverse one and two longitudinal ones.

The transverse cross-section (1) shows a clear presence of individual grinding grooves, with local deformation and FIM deposits, outside the running band at the field side (Fig. 14). The surface roughness disappears to a large extent in the running band, where WEL flakes are embedded in the surface, with locally a tendency to delaminate (Fig. 15).

Concerning deformation directivity at the surface within the running band the following can be observed. At the field side deformation is only very locally present and negligible in magnitude; it is directed toward the field face of the rail and typically a remainder of grinding effects. At the gauge side, surface deformation becomes stronger, but with only a slight directivity toward the gauge face. Also this directivity may typically result from grinding. Only when approaching the gauge corner the deformation gets a clear and consistent directivity toward the gauge face and is related to the wheel-rail contact history. When considering the subsurface crack in the transverse cross-section, any consistent deformation of both crack faces is absent, which indicates that these faces have not transferred major shear stresses (Fig. 16a); however, a strongly increasing deformation, without directivity, of the surface material occurs when approaching the crack mouth at the surface; the thin portion of surface material at this position has

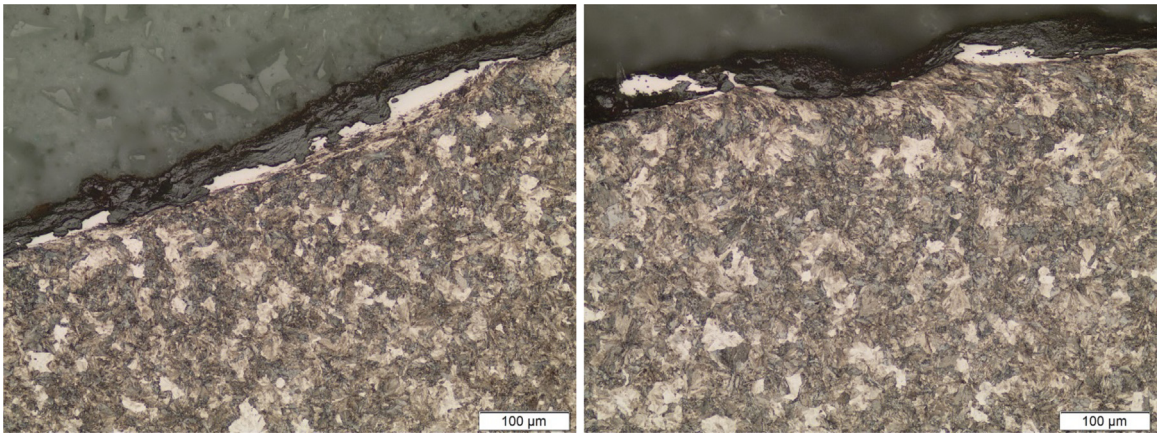

Fig. 14. Grinding grooves with local deformation and FIM deposits at the field side; transverse cross-section (1).

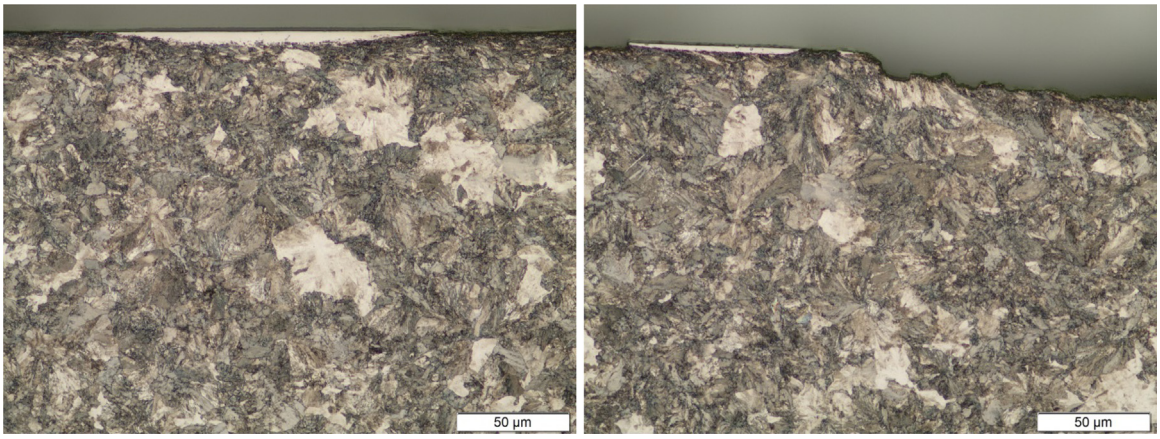

Fig. 15. White etching material embedded in the surface, within the running band (gauge side right); transverse cross-section (1).

Fig. 16. Sub-surface cracking in the transverse cross-section (1): no crack face deformation (a) and flattening of the gauge-side tip of the material portion spalling off (b) (gauge side right).

clearly been flattened by cyclic normal stresses (Fig. 16b).

The longitudinal cross-section (3) along the surface, in the centre of running band and within the spalling zone, shows remainders of grinding grooves (filled with corrosion) along with local deformation, as well as multiple crack initiations at the surface, examples of which are shown in Fig. 17. The surface deformation from the wheel-rail contact history is directed against the running direction, as can be expected in the high rail of a curve. The subsurface crack in the longitudinal cross-section shows a consistent and strong deformation of both crack faces, indicating a transfer of longitudinal shear stresses ('rubbing') in line with the tangential stress history by passing (and notably driven) wheels (Fig. 18) (see also ref. [7], Fig. 7).

Longitudinal Section (2), taken in the gauge corner and outside the spalling zone shows a similar image. There are remainders of grinding grooves, and the subsurface deformation from the wheel-rail contact history is strong, with also at this transverse position a clear directivity against the running direction (Fig. 19).

The microstructural analysis thus confirms the presence and the directivity of the sub-surface plastic strain field induced by the

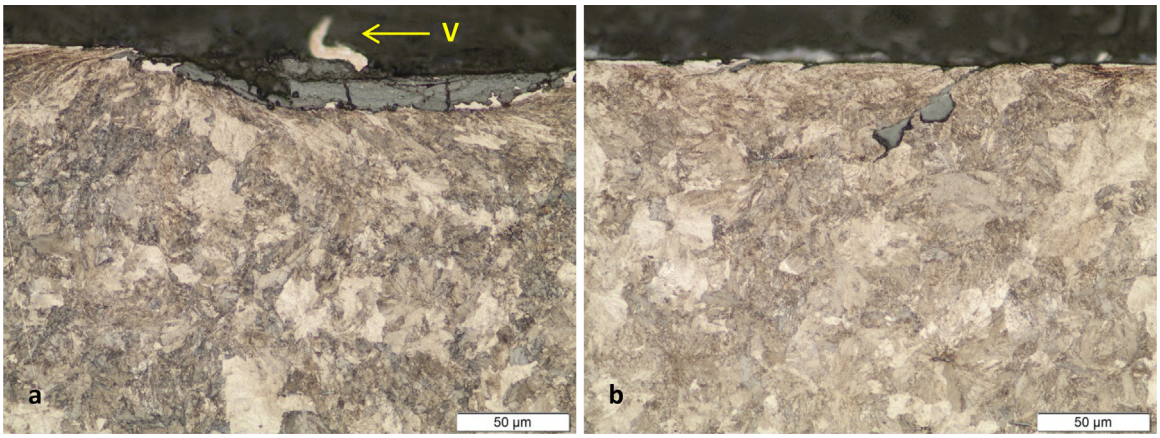

Fig. 17. Longitudinal cross-section (3): remainders of grinding grooves (a) and multiple surface crack initiation (b).

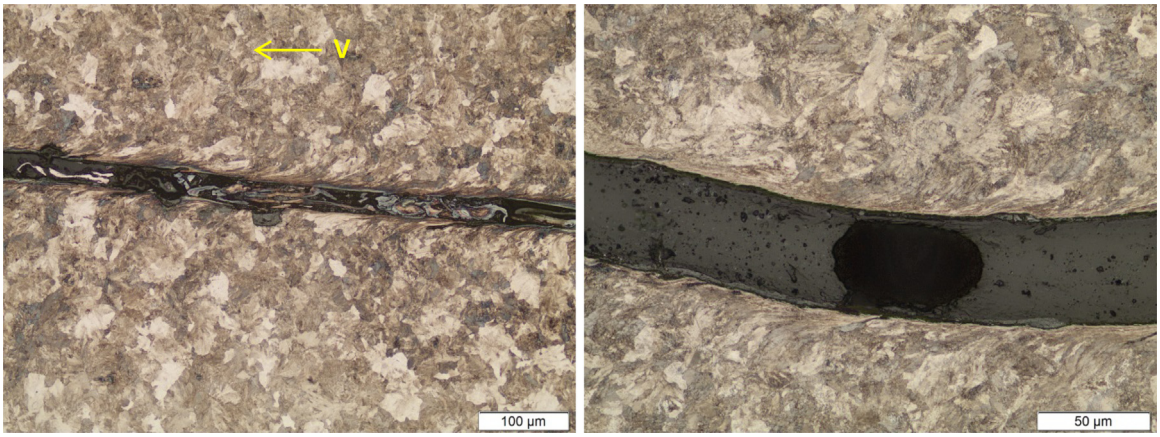

Fig. 18. 'Rubbing' of subsurface crack faces in the longitudinal cross-section (3) indicate significant transfer of longitudinal shear stresses.

wheel-rail contact history, as assumed in the application of the model of Fig. 10 to the defect under consideration. Moreover, the analysis showed the relative dominance of longitudinal tangential stresses to the transverse component for this specific situation. This offers an explanation as to why the crack initiation starts under a relatively small angle with the longitudinal rail axis in Figs. 5 and 11.

6. Final remarks and conclusions

The work presented in this study shows the importance of eventual anisotropy and inhomogeneity of the top layer of the rail for the understanding and modelling of crack growth in the rail surface. In many cases (such as headchecking), cracks in the rail surface are a result of regular RCF, in the sense of a steadily ongoing process of cyclic plastic ratchetting under contact loading. This is typically a high-cycle fatigue process. However, as has been argued in this paper, the apparition of not all surface cracks can be attributed to such a process. The factors that govern their initiation and propagation instead also lead to different crack behaviour. Therefore, models need to take into account these factors in order to explain or predict these particular cracks. In this sense, the recently proposed modelling by Six, Trummer et al. [18,19], who distinguish between 'tribological' (or surface -) and 'global' (or subsurface) plasticity represents a step forward with respect to crack prediction models that start from the initial assumptions of material isotropy and homogeneity.

The main findings of this work can be summarized as follows:

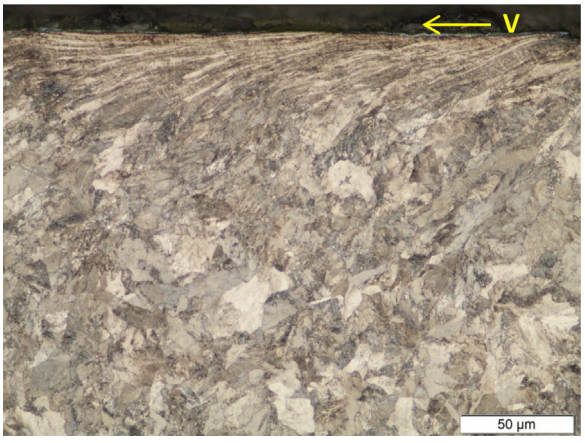

Fig. 19. Subsurface deformation directivity against the running direction; longitudinal cross-section (2).

1) the process of regular RCF, in the sense of ongoing cyclic plastic strain accumulation under contact loading, along with crack initiation usually has as a point of departure:
   i. homogeneity and isotropy of the material in the top layer of the rail, at least at a bulk level;
   ii. coincidence of the nominal and the real wheel-rail contact patch, which excludes (apart from micro-roughness) eventual transient contact stress redistribution within this area;
   iii. stationarity or monotony of the loading regime, which excludes major transitions in parameters describing this operational regime (such as the friction coefficient) over relevant time durations;
2) these three conditions are not generally met in practice;
3) in case of deviation of one of more of these conditions, spalling defects may develop with properties that are distinct from those of 'regular' RCF cracks;
4) a model has been proposed that is able to explain/predict whether a surface-breaking crack develops in the spalling or the transverse defect domain for different track conditions (straight track and curves, upper and lower legs). This model has significant practical relevance, since both domains represent essentially different operational safety risks and require therefore different monitoring and maintenance actions.

Acknowledgements

The work presented in this paper received no industrial or governmental funding, but was undertaken out of curiosity by the author at Delft University of Technology.

References

[1] M. Steenbergen, R. Dollevoet, On the mechanism of squat formation on train rails. Part I: origination, Int. J. Fatigue 47 (2013) 361–372.
[2] M. Steenbergen, R. Dollevoet, On the mechanism of squat formation on train rails. Part II: growth, Int. J. Fatigue 47 (2013) 373–381.
[3] European Norm EN 13674-1, Railway applications - Track - Rail - Part 1: Vignole railway rails 46 kg/m and above (2011).
[4] M. Steenbergen, Rolling contact fatigue in relation to rail grinding, Wear 356–357 (2016) 110–121.
[5] S.L. Grassie, D.I. Fletcher, E.A. Gallardo Hernandez, P. Summers, Studs: a squat-type defect in rails, Proc. Inst. Mech. Eng. F: J. Rail Rapid Transit 226 (2012) 243–256.
[6] S. Grassie, Studs and squats: the evolving story, Wear 366-367 (2016) 194–199.
[7] M. Steenbergen, Squat formation and rolling contact fatigue in curved rail track, Eng. Fract. Mech. 143 (2015) 80–96.
[8] Y. Fujii, K. Maeda, Flaking failure in rolling contact fatigue caused by indentations on mating surface (I): reproduction of flaking failure accompanied by cracks extending bi-directionally relative to the load-movement, Wear 252

(2016) 787–798.
[9] Y. Fujii, K. Maeda, Flaking failure in rolling contact fatigue caused by indentations on mating surface (II): formation process of flaking failure accompanied by cracks extending bi-directionally relative to the load-movement, Wear 252 (2002) 799–810.
[10] Y. Fujii, K. Maeda, Flaking failure in rolling contact fatigue caused by indentations on mating surface (III): mechanism of crack growth in the direction opposite to the load-movement, Wear 252 (2002) 811–823.
[11] A.F. Bower, K.L. Johnson, Plastic flow and shakedown of the rail surface in repeated wheel-rail contact, Wear 144 (1991) 1–18.
[12] K. Dang Van, M.H. Maitournam, On some recent trends in modelling of contact fatigue and wear in rail, Wear 253 (2002) 219–227.
[13] R.I. Carroll, J.H. Beynon, Decarburisation and rolling contact fatigue of a rail steel, Wear 260 (2006) 523–537.
[14] J.E. Garnham, C.L. Davis, Very early stage rolling contact fatigue crack growth in pearlitic rail steels, Wear 271 (2011) 100–112.
[15] M. Itabashi, K. Kawata, Carbon content effect on high-strain-rate tensile properties for carbon steels, Int. J. Impact Eng. 24 (2000) 117–131.
[16] E. Uhlmann, P. Lypovka, L. Hochschild, N. Schröer, Influence of rail grinding process parameters on rail surface roughness and surface layer hardness, Wear 366–367 (2016) 287–293, http://dx.doi.org/10.1016/j.wear.2016.03.023.
[17] S. Pal, C. Valente, W. Daniel, M. Farjoo, Metallurgical and physical understanding of rail squat initiation and propagation, Wear 284–285 (2012) 30–42.
[18] K. Six, A. Meierhofer, G. Trummer, C. Marte, G. Müller, Classification and consideration of plasticity phenomena in wheel-rail contact modeling, Int. J. Railw. Technol. 5 (2016) 55–77.
[19] G. Trummer, K. Six, C. Marte, P. Dietmaier, C. Sommitsch, An approximate model to predict near-surface ratcheting of rails under high traction coefficients, Wear 314 (2014) 28–35.